Authors
S. Parham, H. Li, T.J. Nummy, J.A. Waugh, X.Q. Zhou, J. Griffith, J. Schneeloch, R.D. Zhong, G.D. Gu, and D.S. Dessau

This article is available at CU Scholar: https://scholar.colorado.edu/phys_facpapers/108

Ultrafast Gap Dynamics and Electronic Interactions in a Photoexcited Cuprate Superconductor

S. Parham,[1] H. Li,[1] T. J. Nummy,[1] J. A. Waugh,[1] X. Q. Zhou,[1] J. Griffith,[1] J. Schneeloch,[2] R. D. Zhong,[2] G. D. Gu,[2] and D. S. Dessau[1,3]

[1]*Department of Physics, University of Colorado at Boulder, Boulder, Colorado 80309, USA*
[2]*Condensed Matter Physics and Materials Science Department, Brookhaven National Laboratory, Upton New York, 11973, USA*
[3]*Center for Experiments on Quantum Materials, University of Colorado at Boulder, Boulder, Colorado 80309, USA*

(Received 28 February 2017; revised manuscript received 31 July 2017; published 20 October 2017)

We perform time- and angle-resolved photoemission spectroscopy (trARPES) on optimally doped $Bi_2Sr_2CaCu_2O_{8+\delta}$ (BSCCO-2212) using sufficient energy resolution (9 meV) to resolve the k-dependent near-nodal gap structure on time scales where the concept of an electronic pseudotemperature is a useful quantity, i.e., after electronic thermalization has occurred. We study the ultrafast evolution of this gap structure, uncovering a very rich landscape of decay rates as a function of angle, temperature, and energy. We explicitly focus on the quasiparticle states at the gap edge as well as on the spectral weight inside the gap that "fills" the gap—understood as an interaction, or self-energy effect—and we also make high resolution measurements of the nodal states, enabling a direct and accurate measurement of the electronic temperature (or pseudotemperature) of the electrons in the system. Rather than the standard method of interpreting these results using individual quasiparticle scattering rates that vary significantly as a function of angle, temperature, and energy, we show that the entire landscape of relaxations can be understood by modeling the system as following a nonequilibrium, electronic pseudotemperature that controls all electrons in the zone. Furthermore, this model has zero free parameters, as we obtain the crucial information of the SC gap Δ and the gap-filling strength Γ_{TDoS} by connecting to static ARPES measurements. The quantitative and qualitative agreement between data and model suggests that the critical parameters and interactions of the system, including the pairing interactions, follow parametrically from the electronic pseudotemperature. We expect that this concept will be relevant for understanding the ultrafast response of a great variety of electronic materials, even though the electronic pseudotemperature may not be directly measurable.

DOI: 10.1103/PhysRevX.7.041013

Subject Areas: Nonlinear Dynamics, Strongly Correlated Materials, Superconductivity

I. INTRODUCTION

The study of electronic scattering rates is central to much of modern condensed matter physics, as these scattering rates control or are featured prominently in our understanding of many novel electronic interactions, of electronic transport, optical effects, etc. Scattering rates can, in general, be accessed via the energy domain as widths of various features [1–3] or, more recently, directly in the time domain [4–6]. Naively, it is expected that the scattering rates obtained from the two domains should be very similar or identical, and that those obtained from the time domain might be more precise because the measurements are made directly in the domain of interest. Connecting the two domains has not, however, proven to be straightforward with certain measurements from one domain sometimes orders of magnitude different from that obtained in the other domain [7–9]. Such a serious discrepancy has led to an overall level of confusion and uncertainty in our understanding of both domains for accessing electronic scattering rates and electronic interactions.

The present work spans both domains, allowing us to directly access scattering rates both from measured energy widths and in time, and it does so in a system in which the electronic scattering rates are extremely rich in their behavior as a function of energy, momentum, and temperature. Furthermore, it is a test case in which, for much of the interesting time range, we can simultaneously make a direct measurement of a particularly important quantity—the electronic pseudotemperature [10]. The unique combination

Published by the American Physical Society under the terms of the Creative Commons Attribution 4.0 International license. Further distribution of this work must maintain attribution to the author(s) and the published article's title, journal citation, and DOI.

of all of this information in one system with rich and diverse behavior puts strong constraints on the interpretation and understanding of the data. We therefore believe that our success speaks broadly to its veracity, as well as its potential applicability to many other types of ultrafast experiments and materials systems.

Our experiments were performed on the high-temperature superconductor $Bi_2Sr_2CaCu_2O_{8+\delta}$ (BSCCO-2212). In addition to the general importance of uncovering the physics of high-temperature superconductors, this system is an important test case because with it we not only have access to the superconducting gap states with their myriad of interactions but also to the nodal states that are ungapped. The ability to measure these ungapped nodal states as a function of time delay allows us to directly measure the electronic pseudotemperature—we show that this will be a key parameter as long as we are in the time regime $t > t_{\mathrm{therm}}$, where t_{therm} is the approximate time after which the hot electrons have thermalized with each other (but not necessarily with phonons or the surrounding medium). Such thermalization times will vary from material to material. However, for BSCCO, it is about 200 fs [11], and this is the scale beyond which the electron distribution will have a Fermi-Dirac distribution function (but at a pseudotemperature that may be greatly increased compared to the static system temperature). The ability to directly measure such a distribution is perhaps unique to ultrafast angle-resolved photoemission spectroscopy (ARPES) in a nongapped state, and it is one of the many benefits of this emerging technique.

High temperature superconductors (HTSCs) are a classic example of exotic physics arising from strongly correlated electron systems. Understanding these strong correlations has been a topic of intense research since the inception of HTSC in 1986 [12]. Currently, one of the most powerful tools for investigating these interactions is ARPES, which can probe individual parts of the band structure, and the interaction strengths can be inferred from spectroscopic features such as kinks and line widths [2]. Similarly, the way in which a system responds to an ultrafast perturbation in optical pump-probe experiments is believed to be an excellent method to extract various aspects of electronic interactions, including electron-boson coupling strengths [13–16], SC fluctuations [17,18], and quasiparticle dynamics [19–21]. Combining ARPES with pump-probe techniques, referred to as time-resolved ARPES (trARPES), allows us to investigate a system's response to perturbations while maintaining that crucial momentum selectivity. Here, we show that in the superconducting cuprates, there is rich momentum and energy dependence to the quasiparticle decays, confirming the need for this powerful tool. Furthermore, after a thermalization time, these quasiparticles display "pseudothermal" behavior, and, in fact, the entire landscape of decay rates can be understood within an ultrafast thermal framework.

There have been several previous studies of the cuprates in the time domain [4–7,11,13,19,20,22–35], and they have uncovered rich dynamics; however, they have not come to an agreement about the effects or implications [25,27]. For example, there are trARPES reports of both k-dependent [27] and k-independent [25] quasiparticle decay rates, with interpretations ranging from bimolecular recombination dynamics [6,27] to boson bottleneck scenarios [19,25,36]. Other studies have searched for signatures of Fermi liquidlike behavior in photoexcited quasiparticles [7,37,38], though they have had limited success tying back to Fermi liquid theory. Unfortunately, the behavior of population decay dynamics can be fundamentally different from single-particle dynamics [7], making it challenging to extract singe-particle quantities from pump-probe experiments, especially when the electron thermalization time is short compared to the time resolution [11]. In this regime, it is more appropriate to view the system in terms of excited charge and heat reservoirs whose relaxation determines the system's response. In the cuprate's case, we show that the rate of relaxation of the electronic pseudotemperature (through whatever channel this ultimately decays) is the critical parameter required to understand this rich landscape of decays. Furthermore, the interactions that cause the gap "filling," which are related to the single-particle scattering rates, also follow this electronic pseudotemperature.

II. NODAL DYNAMICS

Figure 1(a) shows an example of the effects of optical pumping on the ARPES spectrum of a cuprate superconductor. The first panel Fig. 1(a) (−1 ps) shows the $T = 25$ K nodal spectrum (where the d-wave superconducting gap is zero) before application of the pump, representing the equilibrium state of the system. All subsequent panels show the same nodal cut but at a variable delay after pumping by 4 μm radiation. There is a large increase in weight above E_F after application of the pump that subsequently decays. By integrating the spectrum in momentum [over a range shown by the yellow arrow in Fig. 1(a)], we can obtain slices of k-local ARPES spectral weight (SW) at every delay—equivalent to the tomographic density of states (TDoS) of Ref. [3] except that the Fermi function has not yet been removed. These SW's are combined into a SW map, as shown in Fig. 1(c), to succinctly show the distribution of SW in both energy and time delay.

The second feature of the pumped spectrum is a loss of weight inside the 70-meV kink scale. This is most clearly seen when we plot the spectral difference, defined as the transient spectrum minus the equilibrium spectrum, as in Fig. 1(b), and the lost spectral weight is represented in red. These transient spectra can be momentum integrated to form a ΔSW map, shown in Fig. 1(d), in direct analog to the SW map discussed above. For the nodal cut, this ΔSW map shows an increase in weight above E_F and a loss

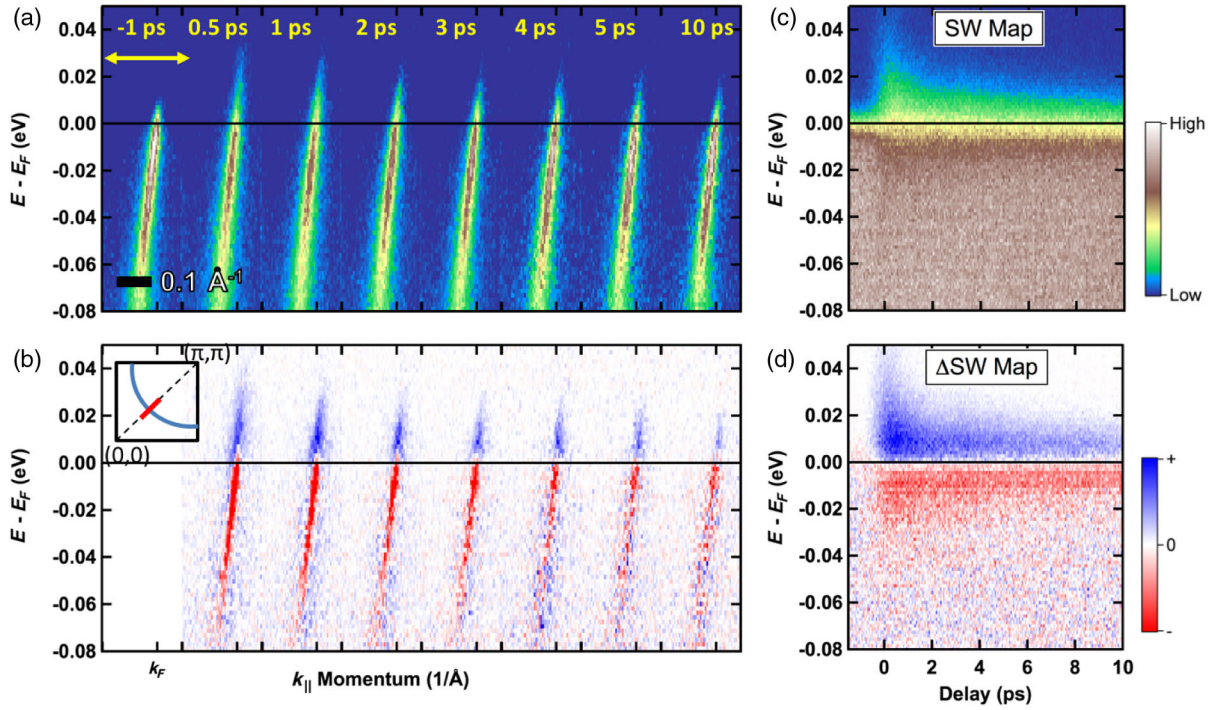

FIG. 1. Nodal response to ultrafast 4-μm pump from an optimally doped, $T_C = 91$ K Bi-2212 sample. Data are taken at the nodal position, shown in the inset to panel (b), at an equilibrium temperature of $T = 25$ K, and a 4-μm pump fluence of 60 μJ/cm^2. Panel (a) shows raw ARPES spectra at various time delays. Panel (b) shows the transient spectra, defined by subtracting the equilibrium spectrum from each delay. Panel (c) shows a map of SW vs delay obtained by integrating the ARPES spectrum along the momentum cut, shown by the yellow arrow in panel (a). Panel (d) is the analogous map for the transient data, referred to as a ΔSW map, produced similarly to panel (c).

below, reflecting the change of electronic temperature with delay. We also observe a chemical potential shift at the node, consistent with previous studies [30], though it is not the focus of our work.

III. OFF-NODAL DYNAMICS

These ΔSW maps are far more interesting when looking at spectra away from the node, which show the effect of the superconducting pairing gaps. Shown in Fig. 2(a) is a near-nodal spectrum at various time delays after pumping. This spectrum, taken at the Fermi surface location indicated by the inset to Fig. 2(b), shows a roughly 12-meV gap and the corresponding bent-back dispersion characteristic of superconductivity. After optical excitation, there is a large increase in occupation above the gap edge, and the spectrum looks similar to the excited nodal spectrum in Fig. 1(a). This excited state subsequently decays, decreasing the weight both inside the gap and above E_F.

A new finding that we report here, made possible by our improved energy resolution compared to previous studies, is that the rate at which the weight decays inside the gap is qualitatively different from that of the weight above E_F. To see this more clearly, we plot the spectral transients in Fig. 2(b). The differential decay is most clear by comparing the transients at 3 and 4 ps, where the in-gap weight visually changes more than the weight above E_F. The differences in the temporal dynamics will be studied in more quantitative detail in the following sections. By 10 ps, the coherent pileup within the 70-meV kink scale has mostly recovered, and there is only a small population of excited Bogoliubov quasiparticles remaining. In Figs. 2(c) and 2(d), we show off-nodal SW and ΔSW maps, produced in the same way as discussed above for the nodal states. Note that in the presence of a gap, the ΔSW zero-crossing is pushed down to $\omega \sim \Delta$ rather than being at E_F like in the nodal case shown in Fig. 1(d). The ω-dependent decay rates are more obvious in Fig. 2(d), where the transition from blue to white below E_F happens before the same transition above E_F. To our knowledge, this unexpected and rich behavior has not been reported before.

IV. ELECTRONIC PSEUDOTEMPERATURE

In order to understand the dynamics in the gapped part of the Fermi surface, we find that it is helpful to quantify the changes to the electron system, namely, the electronic temperature. We do this by fitting the k-integrated ARPES intensity, the spectral weight, to a Fermi distribution and removing the known contribution from the 9-meV experimental energy resolution [39]. These spectral weights,

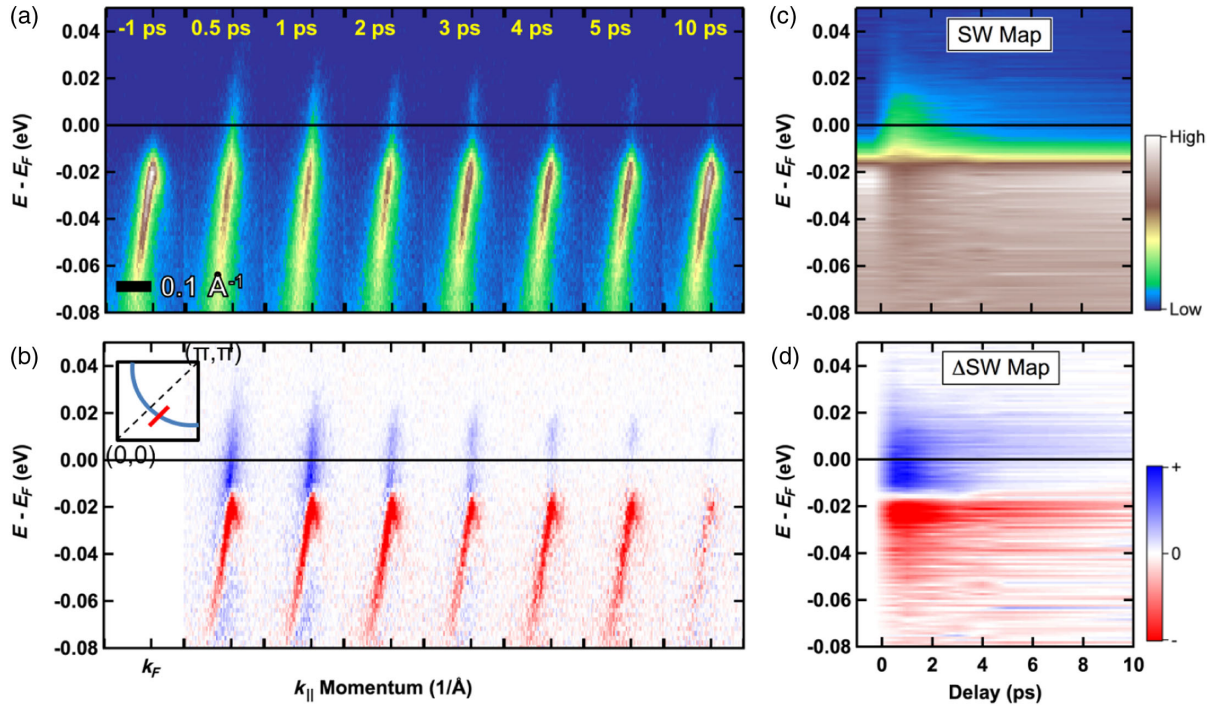

FIG. 2. Off-node [inset to panel (b)] gapped spectra at various pump-probe delays from the same $T_C = 91$ K sample as Fig. 1, with all panels the same as in Fig. 1. The equilibrium temperature is 20 K, and the pump fluence is 80 μJ/cm^2. Note in panel (d) how the region inside the gap recovers (returns to white) faster than the region at the gap edge.

along with their fits, are shown on a log scale in Fig. 3(a) for several delay times. As expected, the electrons follow a Fermi distribution at the time scales measured, which are longer than t_{therm}. Previous optical and trARPES studies have shown that the relevant time scale for near E_F states in the cuprates is 2 ps or slower [21,27]; thus, our 700-fs time resolution is still fast enough to see these decays. Therefore, our system has sufficient time resolution to study the near E_F decays while achieving the energy resolution needed to study the in-gap states. The resulting electronic temperatures are plotted vs delay in Fig. 3(b), where we chose a pump fluence of 45 μJ/cm^2 so that the maximum $T_{el} \sim T_C$. When $T_{el} \leq T_C$, we find that the response follows an exponential decay, and fitting this thermal decay returns a lifetime of approximately 3.7 ± 0.3 ps for the hot electron population.

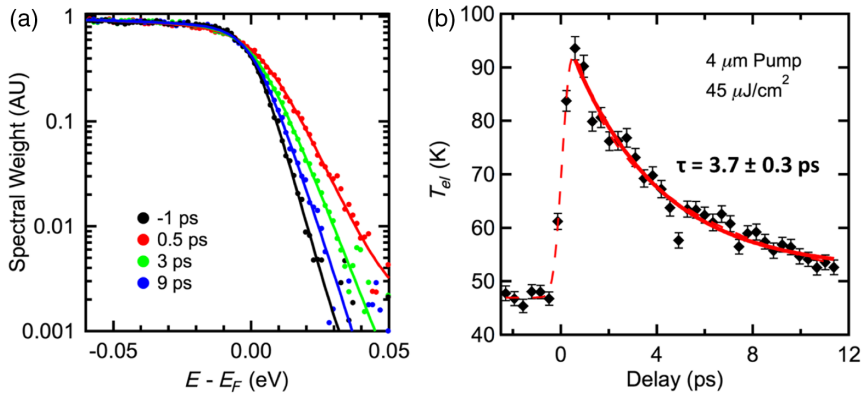

FIG. 3. Extracting electronic temperature from nodal Fermi edges. Panel (a) shows the k-integrated spectral weight for several delays along with Fermi-Dirac fits as solid lines (see Supplemental [39] for details). The momentum integration window is shown by the yellow line in Fig. 1(a). The electronic temperature T_{el} is extracted from the Fermi fit (see Ref. [39]). This T_{el} is plotted vs delay in panel (b) using a 4-μm fluence of 45 μJ/cm^2, which brings the maximum T_{el} to approximately T_C. The temperature decay is fit to a single exponential, shown by the solid red line in panel (b), and the fit returns a decay time of 3.7 ± 0.3 ps. The dashed red line in panel (b) is a guide to the eye.

V. MODELING

In order to understand the energy-dependent temporal dynamics, we make use of the previous result of Perfetti *et al.*, who showed that hot electrons thermalize among themselves within 200 fs after optical excitation [11]. Since we are interested in time windows beyond 200 fs, we can initially consider the electron system as effectively thermalized for all the delays measured, checking later for self-consistency. Note that the electron system can be thermalized with itself while still being out of equilibrium with the underlying lattice, which is what is believed to occur in the first several picoseconds after excitation [11]. If the electrons are thermalized, it will be reasonable to compare the transient time-resolved data to high-resolution equilibrium ARPES measurements, such as those previously measured by our group [3,40].

One of the main results of these previous static ARPES measurements is that the superconducting gap structure in BSCCO is governed by the interplay of the pairing strength Δ and the pair-breaking rate Γ [3]. The gap structure is, to first order, then given by

$$\frac{N_s}{N_n} = \mathrm{Re}\frac{\omega - i\Gamma}{\sqrt{(\omega - i\Gamma)^2 - \Delta^2}} \tag{1}$$

where N_s and N_n are the superconducting and normal-state DOS, respectively, Δ controls the position of the coherence peak, and Γ controls the weight inside the gap. Note that while Γ is itself a representation of the electronic interactions, it can be converted to the standard many-body language via $\Gamma = \Sigma''/Z$, where Σ'' is the imaginary part of the self-energy and Z is the mass renormalization [41]. The static ARPES results show that the temperature dependence of Δ follows a roughly BCS-like behavior, albeit one that closes at a temperature T_{pair} higher than T_C [40]. As shown in Fig. 4(e), for temperatures $T < T_C$, the gap is always greater than about 60% of its low-temperature value. On the other hand, the pair-breaking rate has a very strong temperature dependence in the vicinity of T_C. The exact temperature dependence of Γ changes with doping, but qualitatively, there is always a strong upturn near T_C [40]. When Γ is large relative to Δ, the gap is mostly "filled," which comes with a corresponding decrease in the coherence peak as shown in Fig. 4(f). Therefore, when we combine the strong temperature dependence of Γ with a time-dependent temperature, we expect the weight inside the gap to "unfill" faster than the thermal response.

To model these off-nodal dynamics, we connect to the temperature response measured at the node and the $\Delta(T)$ and $\Gamma(T)$ obtained by high-resolution equilibrium ARPES measurements [40]. At each time delay measured, we assign an electronic temperature based on the nodal data, shown in Fig. 3(b). Next, we use the $\Delta(T)$ and $\Gamma(T)$ curves to define $\Delta(t)$ and $\Gamma(t)$ parametrically and compute the SW

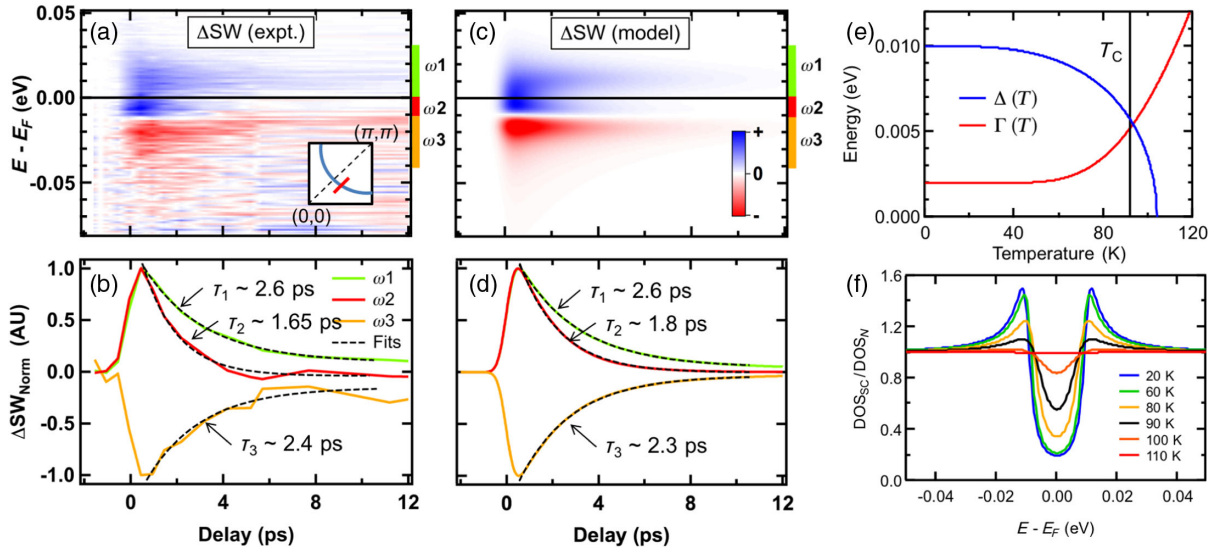

FIG. 4. Ultrafast off-nodal gap and quasiparticle response—data and thermal model. Panel (a) shows the ΔSW map for the cut shown in the inset. Temporal line cuts for different energy regions are shown in panel (b) along with single exponential fits and their returned lifetimes. The energy regions, chosen to improve the counting statistics while still separating the qualitatively different spectral regions, are defined as $-40\ \mathrm{meV} < \omega_3 < -12\ \mathrm{meV}$, $-12\ \mathrm{meV} < \omega_2 < 0\ \mathrm{meV}$, and $0\ \mathrm{meV} < \omega_1 < 30\ \mathrm{meV}$. For clarity, we normalize the temporal line cuts to their maximum values. Panel (c) shows a simulated ΔSW map using our zero-parameter thermal model, discussed in the text. This model, with no free parameters, captures both the qualitative and quantitative features of the experimental data, as shown by the model line cuts in panel (d) (integrated over the same ω ranges) and their associated fitted lifetimes, which match the experimental data well. Panel (e) shows the gap and pair-breaking rate extracted from high-resolution equilibrium ARPES [40] that serve as the input to the thermal model. Panel (f) shows some representative TDoS curves, simulated from the inputs in (e), for which the key effect is the gap principally filling with increasing T.

as the product of a Dynes line shape and the appropriate Fermi distribution, shown in Eq. (2):

$$\mathrm{SW}(t) \equiv \mathrm{Re}\frac{\omega - i\Gamma(t)}{\sqrt{(\omega - i\Gamma(t))^2 - \Delta(t)^2}} \cdot \frac{1}{e^{(\omega-\mu)/kT(t)} + 1} \qquad (2)$$

where $\Gamma(t) \equiv \Gamma(T(t))$ and $T(t)$ is the electronic pseudotemperature vs time. Here, $\Delta(t)$ is defined similarly. The SW curves given by Eq. (2) are then stacked into a SW map. In order to properly take into account the experimental time and energy resolution, we convolve the SW map in energy by a 9-meV Gaussian and in time by a 0.7-ps Gaussian before subtracting the equilibrium SW to obtain the ΔSW map. Finally, we arrive at a ΔSW map analogous to the experimental data, as shown in Fig. 4(c).

At this point, we are ready to compare the data to the simulation. First, note the qualitative agreement between the model and the data, shown together in Fig. 4. We see the extra weight above E_F, shown in blue, and the loss of weight from below the gap scale, shown in red. Also, the zero-crossing (white stripe) occurs at roughly the gap scale, here 12 meV, just as in the data. Finally, the simulation reproduces the faster response of the in-gap electrons, seen as the return to white color by roughly 5 ps for energies within the gap scale. We perform quantitative comparisons between our experimental data and our simulated data by taking identical line cuts from the ΔSW maps and fitting them to exponential decays, shown in Figs. 4(b) and 4(d). Here, we have chosen three energy windows over which to integrate: one from −40 to −12 meV representing the weight lost outside the gap scale, one from −12 meV to E_F representing the in-gap weight, and one from E_F to 30 meV representing the excited quasiparticle weight. We note here that while the superconducting gap function is symmetric with respect to E_F, symmetry is inherently broken by the Fermi distribution; thus, there is little advantage to symmetric integration windows. Because the line cuts have different integration windows, we have plotted them normalized to their peak value. Each trace is fit to a single exponential decay over a range from the peak value to +10 ps, which covers $> 3\tau$ in all cases. The extracted τ's are shown next to the traces, and there is good agreement between data and the model. Therefore, both qualitatively and quantitatively, the thermal model describes the data well, and we can understand the faster in-gap dynamics within this framework.

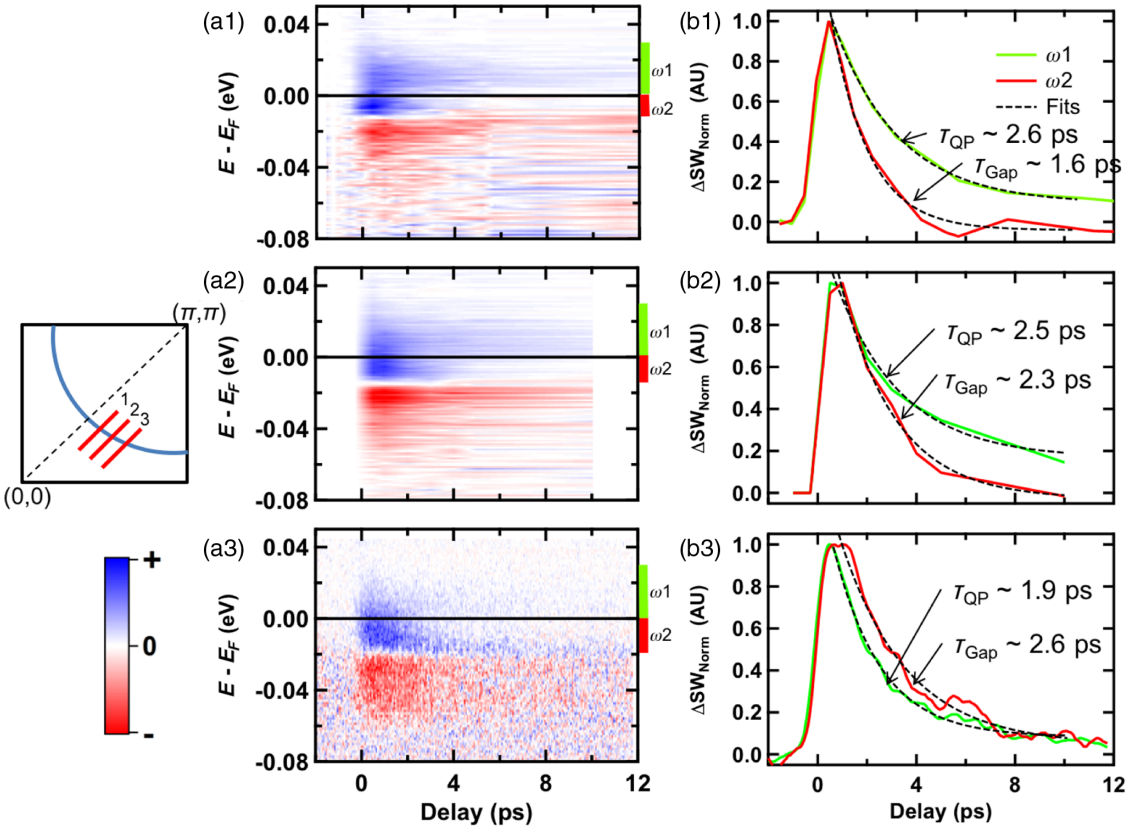

FIG. 5. Off-nodal momentum dependence of ΔSW maps. Panels (a1)–(a3) show ΔSW maps for three different cuts, with k-space locations shown by the inset in panel (a2). Panel (a1) has the same data as Fig. 4(a), reproduced for ease of comparison. Panels (a1)–(a3) have gap sizes of $\Delta = 12$, 15, and 22 meV, respectively. Panels (b1)–(b3) show the temporal line cuts corresponding to each ΔSW map. The integration windows used to generate the line cuts in panel (b) are shown with red and green bars to the right of each ΔSW map. Panels (b1)–(b3) also show single exponential fits in black dashed lines, with extracted τ's indicated in the panels.

One logical extension of this thermal model is to other parts of the Brillouin zone where the superconducting gap has different values. In Fig. 5, we show ΔSW maps for two extra cuts in momentum space with successively larger gap values. These maps are generated in the same fashion as above, and their temporal line cuts are shown in Figs. 5(b1)–5(b3). For ease of comparison with both previous studies and between k-points, we standardize the ω windows as follows: one window from (E_F, 30 meV) representing above E_F quasiparticles [42] and one window from ($-\Delta$, E_F) representing in-gap states. Here, we see rich momentum dependence in the decay dynamics. First, as we move away from the node, the decays above E_F get progressively faster. For the smallest gap size ($\Delta = 12$ meV), the in-gap decay is significantly faster than that above E_F, as discussed above. However, as we move away from the node, this in-gap decay gets *slower*, in contrast to that above E_F, and eventually there is a crossover between the two. This is shown clearly in the progression of line cuts in Figs. 5(b1)–5(b3). This crossover behavior may seem confusing at first, but it arises naturally in the context of our thermal model.

We have performed simulations representing different parts of the zone by changing the equilibrium gap value Δ_{eq} according to the *d*-wave form while keeping Γ and the thermal response the same. This is justified because Γ has been shown to be nearly isotropic in the near-nodal regime studied here [40]. For each Δ_{eq}, we compute the ΔSW map (as discussed above) and take two temporal line cuts, one above E_F and one inside the gap. These line cuts are fit to decaying exponentials, and the extracted lifetimes are compiled with the data in Fig. 6. As shown in Fig. 6, the above E_F decays get faster with increasing off-nodal angle ϕ, while the in-gap decays get slower, achieving a crossover at approximately $\phi = 15°$.

VI. DISCUSSION

Broadly speaking, one can break up the physics into two categories, prethermalization [43] and post-thermalization, i.e., for times less than or greater than t_{therm}. Our study investigates the post-thermalization regime in detail and shows that the relevant parameters for superconductivity, Δ and Γ, follow the electronic pseudotemperature after the thermalization time scale. Previous studies have measured the prethermalization regime and thermalization time scale t_{therm} in detail [11,30,35]. Combining the results of our study, with its improved energy resolution, with others that measure t_{therm} and prethermalized decays gives a coherent picture of the decay dynamics in photoexcited cuprates.

Furthermore, this physics should hold generally for other photoexcited materials. There should be different thermalization times in different compounds, related to quasiparticle decay channels, but, in principle, the post-thermalization decays should follow the pseudotemperature. However, because of experimental or material constraints, it is seldom possible to measure the pseudotemperature directly. In this regard, using trARPES on cuprates is a special test case of this physics because of the rich energy and momentum-dependent decays and the ability to measure the pseudotemperature directly using the superconducting nodal direction.

The momentum dependence of quasiparticle decays is important because that dependence can constrain the possible decay pathways in the system [16]. However, there is currently a debate in the field over whether the quasiparticle decays are *k* independent [25], implying a boson bottleneck [25], or *k* dependent [27], implying a momentum-dependent quasiparticle recombination rate [27]. Another aspect of this debate is whether the superconducting gap Δ recovers at different rates around the

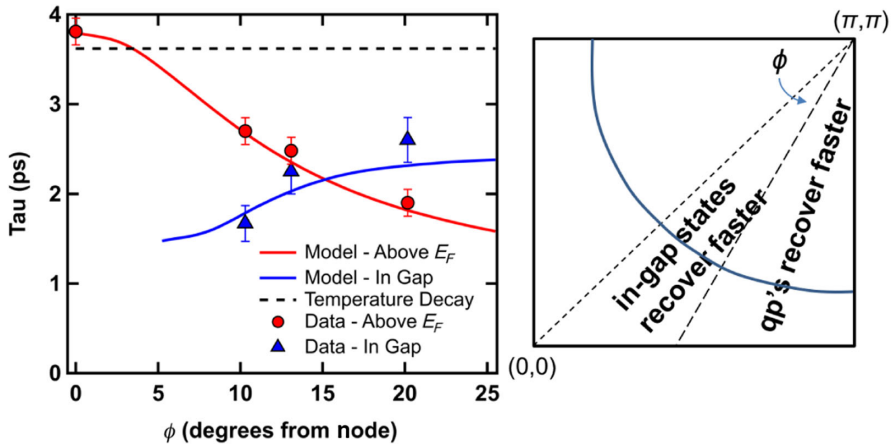

FIG. 6. The *k*-space crossover of gap dynamics. Both experimentally (circles and triangles) and theoretically (solid lines), we find that the near-nodal region is characterized by a faster recovery of in-gap states compared to those above E_F, while the antinodal region shows the reverse. This physics is driven by the interplay of different momentum and temperature-dependent pairing (Δ) and self-energy (Γ) scales. The Fermi surface locations of these regimes are shown in the right panel. The simulated decays (solid lines) represent a model of fully thermalized electrons, with a temperature decay measured via the node (black dashed line), which agrees well with the data.

zone [27] or all at the same rate [31]. An important point here is that all these studies are looking at picosecond scale decays, which are after the thermalization time scale. Our data support the claim that these decay rates are k dependent, though our interpretation is different. In Ref. [27], the authors attribute this behavior to k-dependent quasiparticle recombination dynamics within their own extension of the Rothwarf-Taylor model. Our data and model produce similar behavior; however, all the electrons in the zone are responding to the same thermal decay, and it is just the different gap edges that cause different time dynamics. Furthermore, the general agreement between our data and model implies that, throughout the zone, the superconducting gap recovers according to the thermal response. It is possible that the observed k-independent decays from Ref. [25] are due to worse energy resolution, which would smear out the ω-dependent decays observed here. Therefore, our results resolve this controversy about k-dependent quasiparticle and gap dynamics, and our interpretation is more straightforward than that of Ref. [27].

This thermal model also captures the physics of the decay rate crossover seen in our data, appearing at roughly $\phi = 15°$ in Fig. 6. The good agreement between data and the model suggests that, after t_{therm}, electrons throughout the zone are thermalized; i.e., even quasiparticles optically excited far from the node follow a Fermi-Dirac distribution after t_{therm}. This is consistent with the ability of electron-electron scattering to rapidly redistribute energy within the electron subsystem [35]. Thus, the parameters that determine the overall population decay, Δ and Γ, track the thermalized response, and the electron dynamics throughout the zone can be understood as following from a single control parameter, the electronic pseudotemperature.

VII. IMPLICATIONS

(1) Our findings show that the picosecond scale dynamics in the cuprates, including those inside the gap scale, are dictated by the electronic pseudotemperature. Furthermore, the electronic self-energy follows this transient electronic temperature. This interpretation is consistent with previous results, showing an increase in MDC line width within the kink scale following ultrafast heating [33]. Therefore, a thermalized electron population is an excellent starting reference point for the interpretation of future studies of electron dynamics after t_{therm}. Direct comparison of photoexcited spectra with equilibrium spectra (at the same electronic temperature) can elucidate any higher-order differences caused by optical excitation.

(2) Our study extends the accessible phase space of trARPES experiments using high-energy resolution to peer inside the gap. Here, we have shown that in this newly measured regime, the electron behavior is dictated by the electronic pseudotemperature and by a competition between the two key parameters—the pairing energy scale Δ and the electron scattering rate Γ. These parameters change dramatically as a function of momentum and electronic pseudotemperature, giving rise to a rich landscape of dynamics across momentum and temperature scales, which nonetheless can be readily understood within a simple model with essentially zero free parameters.

(3) Our work connects the single-particle and population lifetimes. The scattering rate Γ is a measure of the single-particle lifetime of the electrons inside the superconducting gap, and we have shown that Γ follows the electronic pseudotemperature. Since the pseudotemperature is a direct measure of the hot electron population, we have shown that single-particle lifetimes can be extracted from population dynamics.

(4) In principle, this thermalization concept should hold for any coupled bosonic subsystems as well. While transient phonon populations have been measured with time-domain THz spectroscopy [45], a technique such as time-resolved Raman spectroscopy (trRaman) could be useful in determining which phonon branches reach an effective bosonic pseudotemperature and on what time scales. Similarly, time-resolved x-ray diffraction could elucidate the behavior of magnetic degrees of freedom [46]. Using trARPES in conjunction with trRaman [47] or these other techniques could determine what role, if any, particular bosons have in moderating cuprate superconductivity.

(5) Our use of MIR pump light paves the way for future experiments exploring or even controlling [48] the superconductivity. In this work, we used 310-meV pump photons specifically because they do not couple strongly to any phonon modes [49], so the main perturbation is to the electronic system. However, it has been suggested [13] that lower-energy pump wavelengths (about 95 meV in YBCO) can resonantly excite the so-called "$2\Delta + \Omega$" mode, which may be important to superconductivity.

VIII. CONCLUSION

We have performed trARPES experiments on optimally doped BSCCO-2212 ($T_C = 91$ K) using a novel pump wavelength and a significantly improved energy resolution over previous works [11,25,27]. With this higher resolution, we can directly track the electronic pseudotemperature in the system by studying the Fermi distribution of the nodal states. In the superconducting state, the thermal response is well described by a single exponential decay, at least out to 12 ps. We observe a rich landscape of quasiparticle population decays, which show strong dependence on both energy and momentum, and can understand this entire landscape by connecting to high-resolution static ARPES data. After the electronic

thermalization time scale, the parameters relevant to superconductivity, Δ and Γ, follow parametrically from the electronic pseudotemperature. This simplifies the interpretation of quasiparticle population dynamics in the post-thermalization regime of the cuprates. We find that the cuprates are an excellent test case of the pseudotemperature concept, given the rich decay landscape and access to the occupation function via the nodal states; therefore, we expect this concept to hold in other photoexcited systems, albeit with a different thermalization time, even if the system or experimental technique precludes an accurate measure of the electronic pseudotemperature.

ACKNOWLEDGMENTS

We would like to thank Tom Devereaux, Ted Reber, and Gerald Arnold for helpful discussions. The work was supported by the NSF Grant No. DMR-1508785, with the equipment purchased in part through NSF Grant No. MRI-1546961. Brookhaven is supported by Department of Energy Contract No. DE-SC0112704. Publication of this article was funded by the University of Colorado Boulder Libraries Open Access Fund.

APPENDIX: METHODS

We perform ARPES measurements in ultrahigh vacuum ($<3E-11$ Torr) with a SPECS Phoibos 225 hemispherical electron analyzer. The samples are high-quality single crystals of optimally doped ($T_C = 91$ K) $Bi_2Sr_2CaCu_2O_{8+\delta}$ grown by a floating zone technique. The sample is cleaved in UHV and typically stored and measured at 45 K, unless stated otherwise. The probe laser is 6.28 eV, and the pump laser is 310 meV; they are generated from a KM Wyvern with TOPAZ OPA/NDFG at 20 kHz. The relative delay between the pump and probe pulses is achieved by a computerized delay stage. More details of the optical generation scheme can be found in Ref. [39]. Because we are interested in studying electron dynamics near the gap scale, we decrease the photon bandwidth (see Ref. [39]) in order to achieve the necessary energy resolution for our study. This gives a combined energy resolution (photons plus analyzer) of 9 meV with a corresponding temporal resolution of 700 fs.

[1] J. Hwang, T. Timusk, and G. D. Gu, *High-Transition-Temperature Superconductivity in the Absence of the Magnetic-Resonance Mode*, Nature (London) **427**, 714 (2004).

[2] A. Damascelli, Z. Hussain, and Z.-X. Shen, *Angle-Resolved Photoemission Studies of the Cuprate Superconductors*, Rev. Mod. Phys. **75**, 473 (2003).

[3] T. J. Reber, N. C. Plumb, Z. Sun, Y. Cao, Q. Wang, K. McElroy, H. Iwasawa, M. Arita, J. S. Wen, Z. J. Xu, G. Gu, Y. Yoshida, H. Eisaki, Y. Aiura, and D. S. Dessau, *The Origin and Non-quasiparticle Nature of Fermi Arcs in* $Bi_2Sr_2CaCu_2O_{8+\delta}$, Nat. Phys. **8**, 606 (2012).

[4] S. G. Han, Z. V. Vardeny, K. S. Wong, O. G. Symko, and G. Koren, *Femtosecond Optical Detection of Quasiparticle Dynamics in High-*t_c $YBa_2Cu_3O_{7-\delta}$ *Superconducting Thin Films*, Phys. Rev. Lett. **65**, 2708 (1990).

[5] R. D. Averitt, G. Rodriguez, A. I. Lobad, J. L. W. Siders, S. A. Trugman, and A. J. Taylor, *Nonequilibrium Superconductivity and Quasiparticle Dynamics in* $YBa_2Cu_3O_{7-\delta}$, Phys. Rev. B **63**, 140502 (2001).

[6] R. A. Kaindl, M. A. Carnahan, D. S. Chemla, S. Oh, and J. N. Eckstein, *Dynamics of Cooper Pair Formation in* $Bi_2Sr_2CaCu_2O_{8+\delta}$, Phys. Rev. B **72**, 060510 (2005).

[7] S.-L. Yang, J. A. Sobota, D. Leuenberger, Y. He, M. Hashimoto, D. H. Lu, H. Eisaki, P. S. Kirchmann, and Z.-X. Shen, *Inequivalence of Single-Particle and Population Lifetimes in a Cuprate Superconductor*, Phys. Rev. Lett. **114**, 247001 (2015).

[8] K. Sugawara, T. Sato, S. Souma, T. Takahashi, and H. Suematsu, *Anomalous Quasiparticle Lifetime and Strong Electron-Phonon Coupling in Graphite*, Phys. Rev. Lett. **98**, 036801 (2007).

[9] I. Gierz, S. Link, U. Starke, and A. Cavalleri, *Non-equilibrium Dirac Carrier Dynamics in Graphene Investigated with Time- and Angle-Resolved Photoemission Spectroscopy*, Faraday Discuss. **171**, 311 (2014).

[10] In this work, we use the prefix "pseudo" as a reminder that we are using an equilibrium concept (temperature) outside of its strictly defined definition.

[11] L. Perfetti, P. A. Loukakos, M. Lisowski, U. Bovensiepen, H. Eisaki, and M. Wolf, *Ultrafast Electron Relaxation in Superconducting* $Bi_2Sr_2CaCu_2O_{8+\delta}$ *by Time-Resolved Photoelectron Spectroscopy*, Phys. Rev. Lett. **99**, 197001 (2007).

[12] J. G. Bednorz and K. A. Müller, *Possible high* T_c *Superconductivity in the Ba-La-Cu-O System*, Z. Phys. B **64**, 189 (1986).

[13] R. A. Kaindl, M. Woerner, T. Elsaesser, D. C. Smith, J. F. Ryan, G. A. Farnan, M. P. McCurry, and D. G. Walmsley, *Ultrafast Mid-infrared Response of* $YBa_2Cu_3O_{7-\delta}$, Science **287**, 470 (2000).

[14] C. Gadermaier, A. S. Alexandrov, V. V. Kabanov, P. Kusar, T. Mertelj, X. Yao, C. Manzoni, D. Brida, G. Cerullo, and D. Mihailovic, *Electron-Phonon Coupling in High-Temperature Cuprate Superconductors Determined from Electron Relaxation Rates*, Phys. Rev. Lett. **105**, 257001 (2010).

[15] M. Sentef, A. F. Kemper, B. Moritz, J. K. Freericks, Z.-X. Shen, and T. P. Devereaux, *Examining Electron-Boson Coupling Using Time-Resolved Spectroscopy*, Phys. Rev. X **3**, 041033 (2013).

[16] C. Giannetti, M. Capone, D. Fausti, M. Fabrizio, F. Parmigiani, and D. Mihailovic, *Ultrafast Optical Spectroscopy of Strongly Correlated Materials and High-Temperature Superconductors: A Non-equilibrium Approach*, Adv. Phys. **65**, 58 (2016).

[17] I. Madan, T. Kurosawa, Y. Toda, M. Oda, T. Mertelj, P. Kusar, and D. Mihailovic, *Separating Pairing from Quantum Phase Coherence Dynamics above the Superconducting Transition by Femtosecond Spectroscopy*, Sci. Rep. **4**, 5656 (2014).

[18] L. Perfetti, B. Sciolla, G. Biroli, C. J. van der Beek, C. Piovera, M. Wolf, and T. Kampfrath, *Ultrafast Dynamics of Fluctuations in High-Temperature Superconductors Far from Equilibrium*, Phys. Rev. Lett. **114**, 067003 (2015).

[19] V. V. Kabanov, J. Demsar, B. Podobnik, and D. Mihailovic, *Quasiparticle Relaxation Dynamics in Superconductors with Different Gap Structures: Theory and Experiments on* $YBa_2Cu_3O_{7-\delta}$, Phys. Rev. B **59**, 1497 (1999).

[20] J. Demsar, R. Hudej, J. Karpinski, V. V. Kabanov, and D. Mihailovic, *Quasiparticle Dynamics and Gap Structure in* $HgBa_2Ca_2Cu_3O_{8+\delta}$ *Investigated with Femtosecond Spectroscopy*, Phys. Rev. B **63**, 054519 (2001).

[21] N. Gedik, M. Langner, J. Orenstein, S. Ono, Y. Abe, and Y. Ando, *Abrupt Transition in Quasiparticle Dynamics at Optimal Doping in a Cuprate Superconductor System*, Phys. Rev. Lett. **95**, 117005 (2005).

[22] P. Kusar, V. V. Kabanov, J. Demsar, T. Mertelj, S. Sugai, and D. Mihailovic, *Controlled Vaporization of the Superconducting Condensate in Cuprate Superconductors by Femtosecond Photoexcitation*, Phys. Rev. Lett. **101**, 227001 (2008).

[23] C. Giannetti, G. Coslovich, F. Cilento, G. Ferrini, H. Eisaki, N. Kaneko, M. Greven, and F. Parmigiani, *Discontinuity of the Ultrafast Electronic Response of Underdoped Superconducting* $Bi_2Sr_2CaCu_2O_{8+\delta}$ *Strongly Excited by Ultrashort Light Pulses*, Phys. Rev. B **79**, 224502 (2009).

[24] M. Beyer, D. Städter, M. Beck, H. Schäfer, V. V. Kabanov, G. Logvenov, I. Bozovic, G. Koren, and J. Demsar, *Photoinduced Melting of Superconductivity in the High-*T_c *Superconductor* $La_{2-x}Sr_xCuO_4$ *Probed by Time-Resolved Optical and Terahertz Techniques*, Phys. Rev. B **83**, 214515 (2011).

[25] R. Cortés, L. Rettig, Y. Yoshida, H. Eisaki, M. Wolf, and U. Bovensiepen, *Momentum-Resolved Ultrafast Electron Dynamics in Superconducting* $Bi_2Sr_2CaCu_2O_{8+\delta}$, Phys. Rev. Lett. **107**, 097002 (2011).

[26] J. Graf, C. Jozwiak, C. L. Smallwood, H. Eisaki, R. A. Kaindl, D. H. Lee, and A. Lanzara, *Nodal Quasiparticle Meltdown in Ultrahigh-Resolution Pump-Probe Angle-Resolved Photoemission*, Nat. Phys. **7**, 805 (2011).

[27] C. L. Smallwood, J. P. Hinton, C. Jozwiak, W. Zhang, J. D. Koralek, H. Eisaki, D.-H. Lee, J. Orenstein, and A. Lanzara, *Tracking Cooper Pairs in a Cuprate Superconductor by Ultrafast Angle-Resolved Photoemission*, Science **336**, 1137 (2012).

[28] W. Zhang, C. L. Smallwood, C. Jozwiak, T. L. Miller, Y. Yoshida, H. Eisaki, D.-H. Lee, and A. Lanzara, *Signatures of Superconductivity and Pseudogap Formation in Nonequilibrium Nodal Quasiparticles Revealed by Ultrafast Angle-Resolved Photoemission*, Phys. Rev. B **88**, 245132 (2013).

[29] W. Zhang, C. Hwang, C. L. Smallwood, T. L. Miller, G. Affeldt, K. Kurashima, C. Jozwiak, H. Eisaki, T. Adachi, Y. Koike, D.-H. Lee, and A. Lanzara, *Ultrafast Quenching of Electron–Boson Interaction and Superconducting Gap in a Cuprate Superconductor*, Nat. Commun. **5**, 4959 (2014).

[30] J. D. Rameau, S. Freutel, L. Rettig, I. Avigo, M. Ligges, Y. Yoshida, H. Eisaki, J. Schneeloch, R. D. Zhong, Z. J. Xu, G. D. Gu, P. D. Johnson, and U. Bovensiepen, *Photoinduced Changes in the Cuprate Electronic Structure Revealed by Femtosecond Time- and Angle-Resolved Photoemission*, Phys. Rev. B **89**, 115115 (2014).

[31] C. L. Smallwood, W. Zhang, T. L. Miller, C. Jozwiak, H. Eisaki, D.-H. Lee, and A. Lanzara, *Time- and Momentum-Resolved Gap Dynamics in* $Bi_2Sr_2CaCu_2O_{8+\delta}$, Phys. Rev. B **89**, 115126 (2014).

[32] C. Piovera, Z. Zhang, M. d'Astuto, A. Taleb-Ibrahimi, E. Papalazarou, M. Marsi, Z. Z. Li, H. Raffy, and L. Perfetti, *Quasiparticle Dynamics in High-Temperature Superconductors Far from Equilibrium: An Indication of Pairing Amplitude without Phase Coherence*, Phys. Rev. B **91**, 224509 (2015).

[33] Y. Ishida, T. Saitoh, T. Mochiku, T. Nakane, K. Hirata, and S. Shin, *Quasi-particles Ultrafastly Releasing Kink Bosons to Form Fermi Arcs in a Cuprate Superconductor*, Sci. Rep. **6**, 18747 (2016).

[34] C. L. Smallwood, R. A. Kaindl, and A. Lanzara, *Ultrafast Angle-Resolved Photoemission Spectroscopy of Quantum Materials*, Europhys. Lett. **115**, 27001 (2016).

[35] J. D. Rameau, S. Freutel, A. F. Kemper, M. A. Sentef, J. K. Freericks, I. Avigo, M. Ligges, L. Rettig, Y. Yoshida, H. Eisaki *et al.*, *Energy Dissipation from a Correlated System Driven out of Equilibrium*, Nat. Commun.**7**, 13761 (2016).

[36] V. V. Kabanov, J. Demsar, and D. Mihailovic, *Kinetics of a Superconductor Excited with a Femtosecond Optical Pulse*, Phys. Rev. Lett. **95**, 147002 (2005).

[37] W. Nessler, S. Ogawa, H. Nagano, H. Petek, J. Shimoyama, Y. Nakayama, and K. Kishio, *Femtosecond Time-Resolved Study of the Energy and Temperature Dependence of Hot-Electron Lifetimes in* $Bi_2Sr_2CaCu_2O_{8+\delta}$, Phys. Rev. Lett. **81**, 4480 (1998).

[38] W. Nessler, S. Ogawa, H. Nagano, H. Petek, J. Shimoyama, Y. Nakayama, and K. Kishio, *Energy Relaxation and Dephasing Times of Excited Electrons in* $Bi_2Sr_2CaCu_2O_8$ *from Interferometric 2-Photon Time-Resolved Photoemission*, J. Electron Spectrosc. Relat. Phenom. **88–91**, 495 (1998).

[39] See Supplemental Material at http://link.aps.org/supplemental/10.1103/PhysRevX.7.041013 for details on the optical generation scheme, data fitting procedures, and pseudothermal simulation.

[40] T. J. Reber, N. C. Plumb, Y. Cao, Z. Sun, Q. Wang, K. McElroy, H. Iwasawa, M. Arita, J. S. Wen, Z. J. Xu *et al.*, *Prepairing and the "Filling" Gap in the Cuprates from the Tomographic Density of States*, Phys. Rev. B **87**, 060506 (2013).

[41] Gerald Arnold (private communication).

[42] While the interval (E_F, 30 meV) contains some in-gap states, the qualitative behavior of the above E_F states, with respect to their temporal and momentum dependence, is similar. Please see Ref. [39] for details.

[43] We are using the term "prethermalization" in reference to times before electronic thermalization, i.e., for times $0 < t < t_{\mathrm{therm}}$. This is distinct from the term's usage in the literature of isolated quantum systems, where it describes a particular regime of relaxation dynamics in nonequilibrium quantum systems [44].

[44] J. Berges, Sz. Borsányi, and C. Wetterich, *Prethermalization*, Phys. Rev. Lett. **93**, 142002 (2004).

[45] A. Pashkin, M. Porer, M. Beyer, K. W. Kim, A. Dubroka, C. Bernhard, X. Yao, Y. Dagan, R. Hackl, A. Erb *et al.*, *Femtosecond Response of Quasiparticles and Phonons in Superconducting* $YBa_2Cu_3O_{7-\delta}$ *Studied by Wideband Terahertz Spectroscopy*, Phys. Rev. Lett. **105**, 067001 (2010).

[46] H. Ehrke, R. I. Tobey, S. Wall, S. A. Cavill, M. Först, V. Khanna, Th. Garl, N. Stojanovic, D. Prabhakaran, A. T. Boothroyd *et al.*, *Photoinduced Melting of Antiferromagnetic Order in* $La_{0.5}Sr_{1.5}MnO_4$ *Measured Using Ultrafast Resonant Soft X-Ray Diffraction*, Phys. Rev. Lett. **106**, 217401 (2011).

[47] J.-A. Yang, S. Parham, D. Dessau, and D. Reznik, *Novel Electron-Phonon Relaxation Pathway in Graphite Revealed by Time-Resolved Raman Scattering and Angle-Resolved Photoemission Spectroscopy*, Sci. Rep. **7**, 40876 (2017).

[48] D. Nicoletti, E. Casandruc, Y. Laplace, V. Khanna, C. R. Hunt, S. Kaiser, S. S. Dhesi, G. D. Gu, J. P. Hill, and A. Cavalleri, *Optically Induced Superconductivity in Striped* $La_{2-x}Ba_xCuO_4$ *by Polarization-Selective Excitation in the Near Infrared*, Phys. Rev. B **90**, 100503 (2014).

[49] S. Tajima, T. Ido, S. Ishibashi, T. Itoh, H. Eisaki, Y. Mizuo, T. Arima, H. Takagi, and S. Uchida, *Optical-Phonon Study of Single Crystals of Various Layered Cuprates and Related Materials: Evidence of Unique Electron-Phonon Coupling in the* CuO_2 *Plane*, Phys. Rev. B **43**, 10496 (1991).